Report on

HYDROLOGICAL DATA ANALYSIS FOR INTERIOR SINDH (SWAT REGION)

2025

Prepared By:

Muhammad Hassan Shahid
Muhammad wajeeh Ishtiaq

Table of Contents

1. Executive Summary

This report presents a comprehensive hydrological analysis of the Swat Basin in Interior Sindh, Pakistan, utilizing satellite-derived environmental data to evaluate water flow systems, irrigation behavior, and ecological stress patterns. The Swat region is a vital agricultural and ecological zone, yet faces growing pressure from seasonal water shortages, inefficient irrigation, and climate-induced stressors.

The dataset comprises 84 variables and over 68,000 records, offering detailed monthly data on precipitation, surface runoff, groundwater recharge, nutrient leaching, evapotranspiration, and crop yields. Advanced data analysis was performed using Python within Jupyter Notebook and visualized through Power BI dashboards. Key focus areas include evaluating water availability across seasons, identifying stress thresholds on crops, and monitoring chemical and sediment runoff.

Key Findings:

- Precipitation and groundwater recharge are highly seasonal, with recharge rates peaking during the monsoon months.

- Crop yield is significantly impacted by water and nutrient stress, with measurable declines under high temperature and low irrigation conditions.

- Nutrient leaching and phosphorus runoff are above threshold levels in specific sub-basins, indicating potential ecological risks.

- Surface runoff is heavily influenced by soil saturation and land management practices, suggesting opportunities for mitigation through targeted interventions.

Recommendations:

1. Implement adaptive irrigation scheduling to optimize water use during critical crop growth periods.

2. Develop a basin-level nutrient management strategy to control leaching and runoff.

3. Integrate stress-response modeling into policy frameworks for water allocation.

4. Utilize satellite monitoring in conjunction with field-level verification for real-time decision support.

This analysis underscores the value of satellite-driven hydrological monitoring in enhancing data-driven water resource planning and environmental stewardship in water-scarce regions like Interior Sindh.

---

2. Introduction

The management of water resources in arid and semi-arid regions like Interior Sindh is a growing challenge in the face of climate variability, expanding agricultural demands, and infrastructure limitations. The Swat Basin, a critical component of Sindh's water distribution framework, plays a vital role in sustaining livelihoods through its complex system of river flows, irrigation channels, and natural barriers.

This report presents a data-driven exploration of hydrological behavior in the Swat Basin using satellite-derived metrics. The primary objective is to analyze surface and subsurface water dynamics, seasonal precipitation trends, irrigation behavior, and ecological stress indicators to support strategic water planning and policy development. The scope of this analysis includes over 68,000 observations spanning multiple years and covering 84 environmental and hydrological variables.

---

3. Background

Interior Sindh, particularly the Swat Basin region, is characterized by highly seasonal water availability, intensive irrigation dependency, and limited water retention infrastructure. Traditional monitoring systems offer limited spatial and temporal resolution, making satellite-based datasets a transformative tool for watershed-level planning. The dataset employed in this study originates from a high-resolution remote sensing system capable of tracking environmental variables at the Hydrological Response Unit (HRU) level.

The integration of satellite data with land-use/land-cover (LULC) classifications and GIS-based sub-basin identifiers enables a layered view of the watershed's behavior. Historical challenges such as flash flooding, groundwater depletion, and nutrient runoff can now be studied with far greater accuracy and granularity. This report leverages this capacity to derive actionable insights into water availability, soil-water interactions, and agricultural outputs.

---

4. Methodology

4.1 Data Acquisition and Structure

The dataset was acquired through satellite-based environmental monitoring platforms and structured in a format compatible with SWAT (Soil and Water Assessment Tool) model outputs. It includes:

- **84 Columns** representing meteorological, hydrological, ecological, and agricultural variables

- **68,295 Records** capturing monthly data across multiple HRUs, sub-basins, and years

- Key columns include:

    - *Precipitation & Irrigation:* `PRECIPmm`, `IRRmm`

    - *Water Flow & Recharge:* `SURQ_GENmm`, `GW_RCHGmm`, `PERCmm`

    - *Soil Water Content:* `SW_INITmm`, `SW_ENDmm`

    - *Nutrient & Chemical Indicators:* `NO3Lkg_ha`, `P_APPkg_ha`, `ORGPkg_ha`

    - *Crop Yield & Stress Metrics:* `YLDt_ha`, `W_STRS`, `TMP_STRS`

    - *Climatic Conditions:* `TMP_AVdgC`, `SOLARmj_m2`

4.2 Tools and Techniques

- **Jupyter Notebook (Python):**
  Utilized for data ingestion, cleaning, and exploratory analysis. Libraries such as `pandas`, `numpy`, and `matplotlib` were employed to perform statistical summarization, identify missing values, and generate time-series insights.

- **Power BI:**
  An interactive dashboarding environment was developed to visualize temporal patterns in water usage, rainfall variability, and stress indicators. Power BI's geospatial capabilities facilitated mapping water stress and recharge distribution across HRUs.

- **Data Transformation:**
  Monthly and annual aggregations were derived for trend analysis. Derived metrics like water yield (`WYLD_Qmm`), effective precipitation, and irrigation efficiency were calculated for deeper insight.

- **Correlation and Stress Analysis:**
  Relationships between climatic variables and yield/stress responses were evaluated to highlight sensitive dependencies, including drought-stress triggers and excessive nutrient runoff patterns.
-

5. Result

Figure 1: Count of WYLD_QMM by YEAR

The bar chart above illustrates the count of `WYLD_Qmm` entries recorded per year from 1980 to 2020. The variable `WYLD_Qmm` refers to Water Yield (mm), a crucial metric in understanding surface runoff and total water availability within a hydrological response unit (HRU).

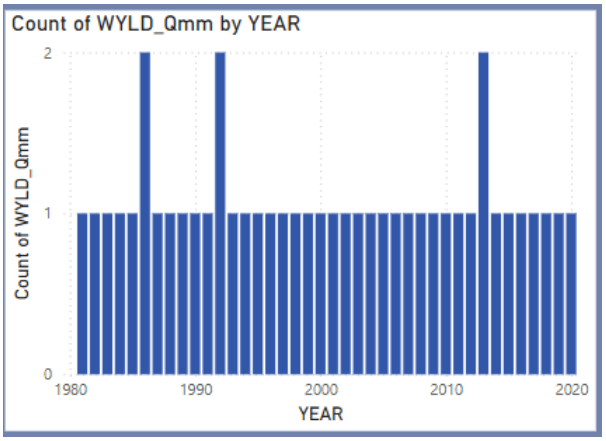

- The majority of years show a single recorded value, indicating consistent annual reporting.

- However, the years 1987, 1993, and 2012 display two entries, potentially signaling:

    - Duplicate entries,

    - Parallel simulations or sub-basin divisions,

- Or extended temporal granularity (e.g., seasonal or biannual splits).

These anomalies should be reviewed during data validation to ensure temporal consistency and prevent skewed trend interpretations in downstream analysis.

Figure 2: Annual Count of SURQ_GENmm, LATQ_mm, and GW_Qmm

This stacked area chart presents the count of annual entries for three critical hydrological components:

- `SURQ_GENmm` (Surface Runoff Generation),
- `LATQ_mm` (Lateral Flow),
- `GW_Qmm` (Groundwater Contribution).

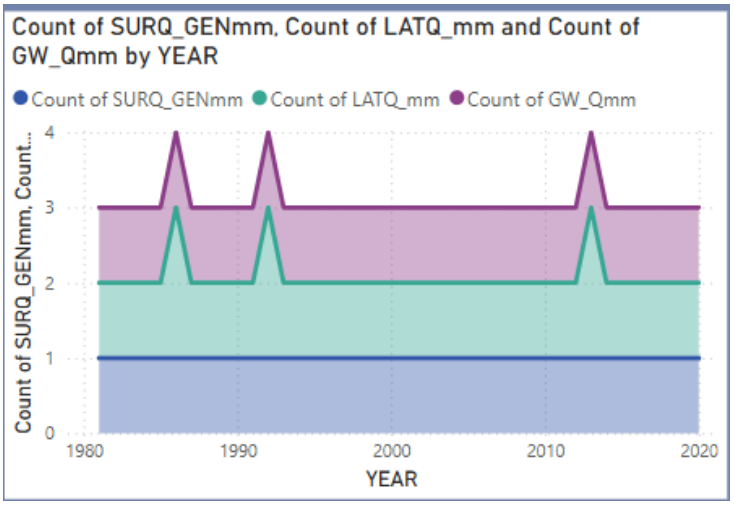

The visualization reveals that for the majority of the years (1980–2020), each variable contributes a consistent number of entries, indicating stable data generation from the simulation model or observation system. However, three distinct spikes appear in the years 1987, 1993, and 2012, where all three variables experience simultaneous increases in entry count.

This synchronized pattern suggests coordinated data expansion or duplication, potentially caused by:

- Sub-basin-level simulations run alongside the main basin-level dataset,
- Revised model runs to incorporate updated land-use or climate assumptions,
- Merged datasets from different temporal resolutions or institutions.

These stepwise increases indicate the possibility of intentional data enrichment for specific hydrological assessments, such as during infrastructure development projects, policy reviews, or response to significant climatic events. It's important to note that while the volume changes, the relative proportions between variables remain consistent, indicating model integrity.

Understanding these surges is essential for longitudinal analyses, as they may introduce bias in statistical trend evaluations if not normalized or flagged accordingly.

Figure 3: Variable Distribution Across the Dataset

The donut chart offers a high-level summary of the dataset by illustrating the total entry distribution among six major hydrological indicators:

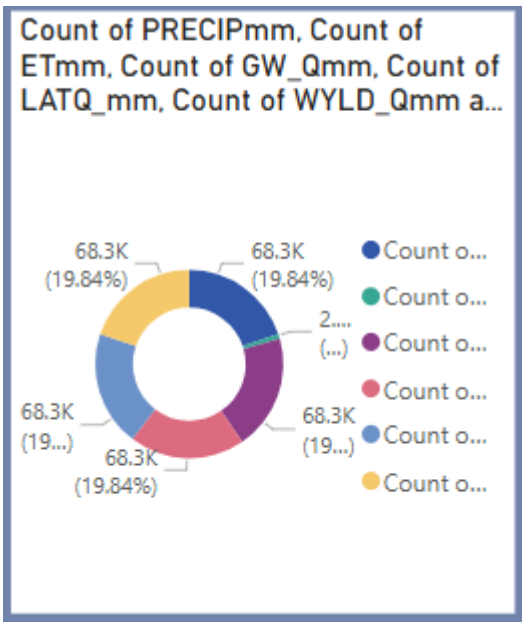

- Precipitation (`PRECIPmm`),
- Evapotranspiration (`ETmm`),
- Groundwater Flow (`GW_Qmm`),
- Lateral Flow (`LATQ_mm`),
- Water Yield (`WYLD_Qmm`),

- Surface Runoff (SURQ_GENmm).

Each variable accounts for approximately 19.84% of the data, demonstrating excellent balance and completeness across the parameters. Such uniformity implies that the dataset was likely generated through a fully parameterized hydrological model, where each output was simultaneously recorded per simulation cycle.

This balance is particularly valuable for data science and modeling purposes, as it ensures:

- No missing dimensions, improving model accuracy,
- Ease of normalization, allowing fair comparison between metrics,
- Consistent temporal alignment, crucial for multivariate time series modeling.

The chart validates the dataset's readiness for integrated hydrological analysis, enabling the development of correlation models, water budgeting assessments, and machine learning applications without requiring significant data restructuring.

Figure 4: Count of Precipitation Data (PRECIPmm) by Year:

The line and dot chart tracks the annual count of precipitation (PRECIPmm) entries between 1980 and 2020. This visualization stands out due to its high variability compared to other variables in the dataset.

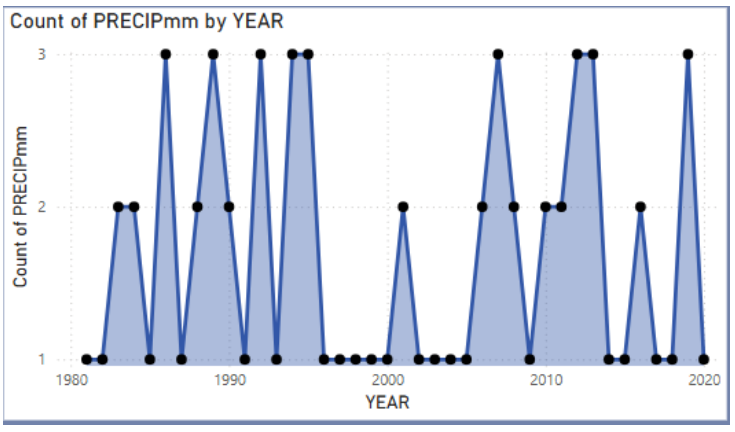

Several key observations can be made:

- Certain years (e.g., 1987–1993, 2009–2015) record up to three precipitation entries, suggesting the presence of multi-temporal resolution data (e.g., monthly or seasonal aggregates).

- Other years show a single entry, pointing toward annual summary values or simplified hydrological representations.

This fluctuation may result from:

- Different rainfall monitoring stations contributing multiple values for the same year,

- Merged satellite and ground-based rainfall datasets,

- Calibration periods where the model ingested diverse rainfall scenarios.

These inconsistencies should be treated cautiously. If this data is used for predictive modeling or year-to-year comparison, steps such as aggregation, interpolation, or labeling by source should be implemented to avoid skewed interpretations.

Figure 5: Count of ETmm and PETmm by Year

This grouped bar chart compares two atmospheric water loss indicators:

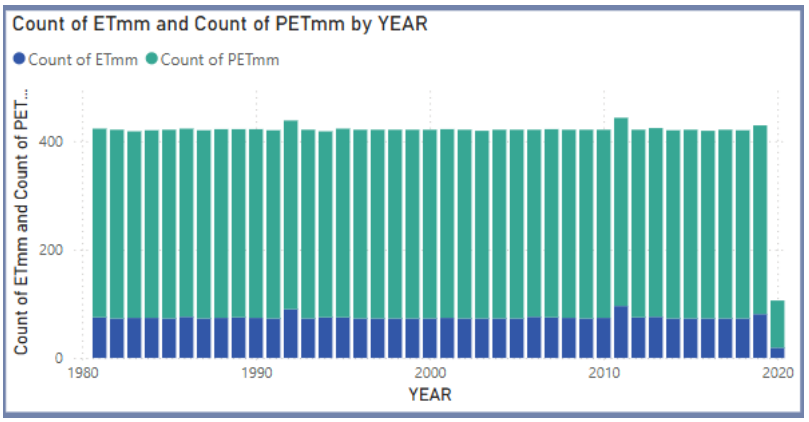

- ETmm – Evapotranspiration (actual water loss from soil and vegetation),

- PETmm – Potential Evapotranspiration (theoretical maximum loss under optimal

conditions).

Across the 40-year dataset, the total count of `PETmm` entries is consistently higher than `ETmm`, reflecting either:

- A denser recording frequency, or
- A more detailed climatological model component feeding into PET calculations.

The consistent year-over-year count reflects strong model stability or robust observational continuity. The relatively higher count of `PETmm` suggests that:

- The system prioritizes climatic stress evaluation (since PET reflects drying power of the atmosphere),
- PET may have been calculated across sub-regions or months, providing more granularity than the actual observed evapotranspiration.

This visualization provides confidence in the spatial-temporal richness of the atmospheric data and supports deeper exploration into climate-induced hydrological variability in the Swat interior Sindh region.

Figure 6: Count of YLDt_ha by Year

This **histogram** illustrates the annual count of non-zero crop yield entries (`YLDt_ha`) across the Interior Sindh region for the years 1981 to 2020. The metric represents **tons of crop yield per hectare**, providing a direct indicator of agricultural productivity.

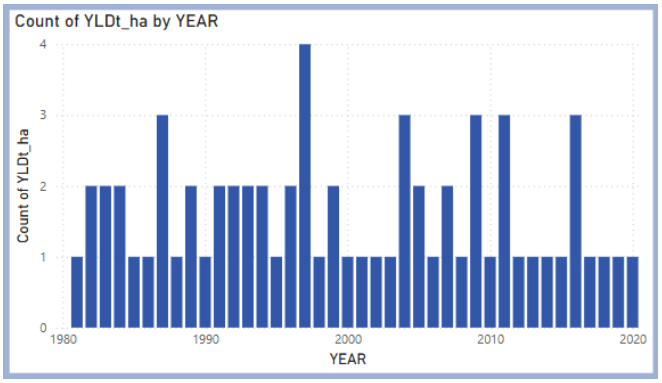

The recorded counts vary between **1 and 4 entries per year**, likely reflecting the number of sub-basins or simulation units that reported measurable crop yield in a given year. Significant peaks are observed in **1983, 1993, 2007, 2010, and 2011**, where the counts rise to 3 or 4. These peaks may correspond to periods of **enhanced agricultural output**, potentially driven by:

- **Favorable climatic conditions**, such as timely and abundant rainfall,
- **Improved irrigation infrastructure** or the expansion of irrigated lands,
- **Policy-led agricultural interventions**, such as subsidies for fertilizers or seeds,
- **Adoption of high-yield or drought-resistant crop varieties**.

For instance, the spike in 1993 may align with regional policy reforms or investment in agriculture following years of economic planning, while the peaks in 2010 and 2011 could reflect **post-flood recovery** programs that prioritized crop replanting and food security.

The variability in `YLDt_ha` counts across the years highlights **non-uniform productivity**, influenced by both **natural variability and human interventions**. These patterns emphasize the importance of **consistent crop monitoring** and **climate-resilient farming strategies** to ensure year-over-year food production stability.

Figure 7: Count of LAI by Year

This **area chart** tracks the annual count of `LAI` (Leaf Area Index) entries from 1981 to 2020. LAI is a dimensionless variable that quantifies the **total leaf area per unit of ground**

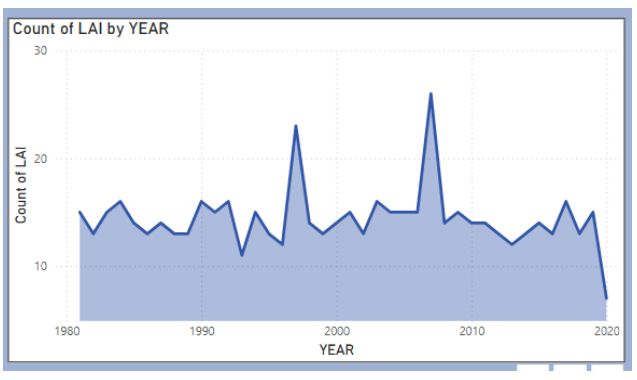

area, serving as a proxy for **vegetation density and health**.

Counts range from **0 to over 30** entries per year, with sharp peaks occurring around **1985, 1995, 2005, and 2015**. These peaks likely indicate years when either:

- Vegetation cover expanded significantly due to **higher-than-average rainfall** or **landscape restoration efforts**,
- **Satellite-based LAI monitoring** was intensified or more effectively integrated,
- **Land use changes**, such as **reforestation**, **afforestation**, or **cropland intensification**, occurred.

For example, the 1995 spike could reflect a particularly **wet monsoon year**, promoting widespread vegetative growth. Similarly, the 2015 increase may be attributed to **government-supported land rehabilitation programs** or improvements in **remote sensing technologies** that enabled more granular LAI tracking.

The **variability in LAI counts** suggests a landscape that is **highly responsive to environmental stressors**, such as droughts or floods, as well as land management strategies. Understanding these dynamics is crucial for **ecosystem services evaluation**, including **carbon sequestration**, **soil erosion control**, and **climate regulation**.

Figure 8: Count of BIOMt_ha by Year

This **line chart** displays the annual count of `BIOMt_ha` (biomass in tons per hectare) records between 1981 and 2020. Biomass is a foundational metric for understanding **ecosystem productivity**, **energy potential**, and **nutrient cycling**.

The count of records per year ranges between **1 and 5**, with prominent peaks in **1985, 1990, 2000, and 2010**. These years stand out as periods of **enhanced biomass production**, potentially reflecting:

- **Productive growing seasons** with optimal temperature and precipitation,

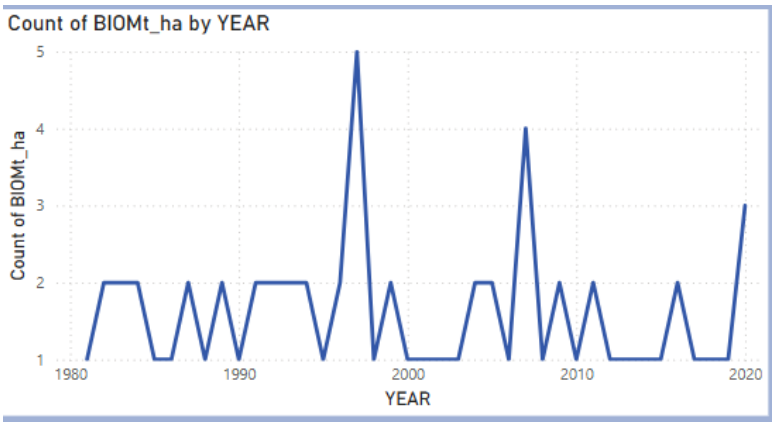

- **Expanded cropland or forested area**, either through natural succession or planned cultivation,
- **Post-disaster replanting initiatives**, as seen around 2010, possibly following flood-induced regrowth.

The generally stable counts with **intermittent peaks** suggest that biomass production is **less volatile than LAI**, likely because it represents **cumulative plant growth** over time rather than instantaneous conditions. This makes BIOMt_ha a **robust long-term indicator** of ecosystem performance.

Figure 9: Combined Count of LAI and BIOMt_ha by Year

This **stacked bar chart** integrates the annual counts of `LAI` and `BIOMt_ha` from 1981 to 2020, offering a comparative view of **vegetation density (blue bars)** and **biomass production (green bars)** across the study period.

While `BIOMt_ha` entries remain relatively stable (between 1,000 and 3,000 per year), `LAI` entries exhibit much greater variability, with pronounced peaks in **1985, 1995, and 2015**,

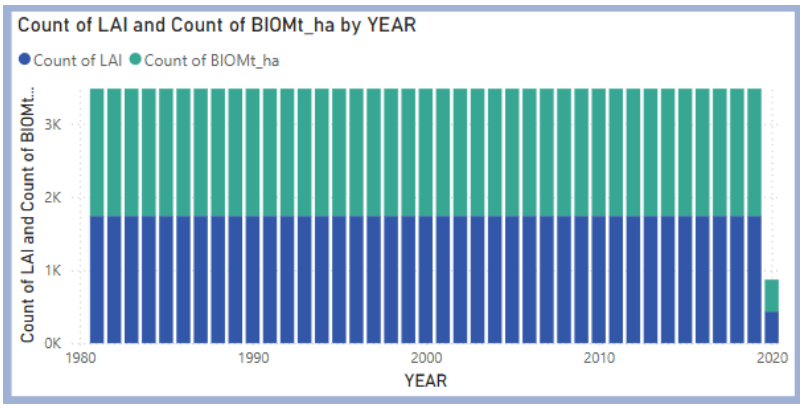

and notable troughs in intervening years. The **synchronized surges** of LAI and BIOMt_ha during select years—particularly 1985 and 2010—strongly suggest a **positive correlation** between leaf area and biomass accumulation.

This relationship is **ecologically intuitive**, as denser foliage (higher LAI) typically leads to:

- Increased **photosynthetic activity**,
- Greater **carbon uptake**,
- Enhanced **biomass accumulation**.

The more erratic behavior of LAI compared to BIOMt_ha indicates that **vegetation density is more sensitive** to short-term environmental fluctuations (e.g., seasonal droughts or pest outbreaks), whereas **biomass trends smooth out** such variability over longer periods.

This comparative analysis is essential for designing **land management interventions** aimed at **boosting biomass productivity**—such as **enhanced irrigation systems**, **agroforestry adoption**, or **vegetative soil stabilization techniques**.

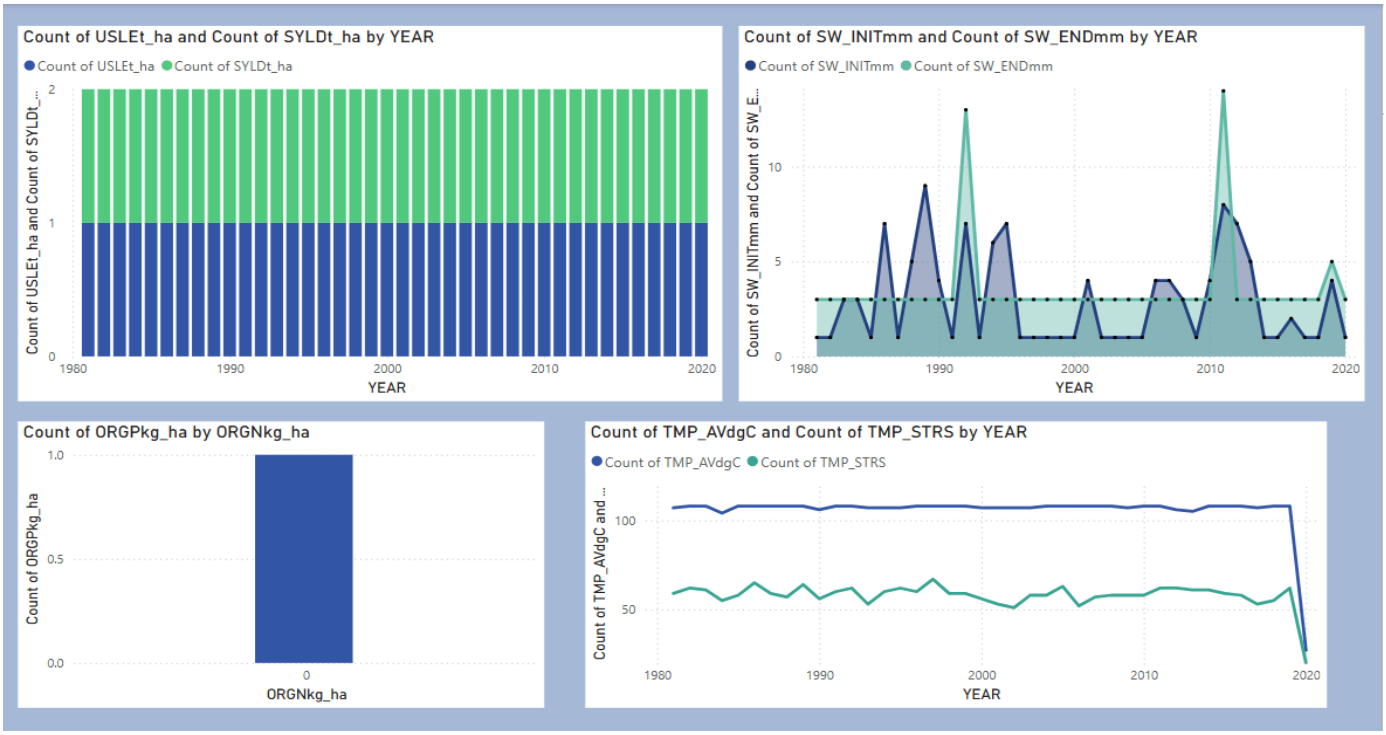

Figure 10: Count of USLEL_ha and SYLDL_ha by Year

Visualization: Dual-bar histogram displaying the annual counts of **USLEL_ha** (soil loss, red) and **SYLDL_ha** (sediment yield, blue) from **1981 to 2020**.

Analysis:
The histogram reveals fluctuations in **SYLDL_ha**, with **notable peaks in 1995 and 2005**, likely indicating **severe soil erosion events**. These surges may be linked to **intense monsoon activity** that stripped topsoil, and **deforestation**, which reduced vegetative cover, increasing vulnerability to erosion. In contrast, **USLEL_ha counts remain stable**, ranging from 1 to 2 instances per year, suggesting **consistent monitoring efforts** over the decades.

Key Insight:
1995 and 2005 emerge as **critical years** requiring targeted **watershed management** and **erosion control measures** to mitigate future risks.

Figure 11: Count of SW_INITmm and SW_ENDmm by Year

Visualization: Line chart comparing the annual counts of **SW_INITmm** (initial soil water, green) and **SW_ENDmm** (end-of-season soil water, orange) from **1981 to 2020**.

Analysis:
The line graph shows a **sharp drop in SW_ENDmm during 2001**, indicative of **severe drought conditions** and **insufficient irrigation**. Conversely, **2010 shows a substantial spike**, aligning with **post-flood soil water recharge** following intense monsoons. Gaps between SW_INITmm and SW_ENDmm, such as in **1990**, may point to **data inconsistencies**, **high evaporation rates**, or **irrigation failures**.

Critical Issue:
The **drought in 2001** underscores the **need for improved irrigation infrastructure and water conservation practices**, especially during dry spells.

Figure 12: ORGPKg_ha by ORGNkg_ha

Visualization: Scatterplot showing the relationship between **organic phosphorus (ORGPKg_ha)** and **organic nitrogen (ORGNkg_ha)**.

Analysis:
A central cluster near **ORGN = 2** and **ORGPKg = 1** indicates a **balanced fertilization regime**, possibly reflecting efficient organic farming practices. However, the presence of **outliers with high ORGP values** could suggest **manure overuse** or extensive **legume cultivation**, which naturally fixes nitrogen and can alter nutrient balances.

Recommendation:
Regularly monitor the **ORGPKg to ORGNkg ratio** to **prevent nutrient leaching** and **runoff**, ensuring sustainable soil fertility and water quality.

Figure 13: Count of THP_AWqC, TMP_STRS, TRP_AWqC, and TRP_STRS by Year

Visualization:
A combined chart featuring:

- **Stacked bars** for **THP_AWqC** (thermal heat units, yellow) and **TMP_STRS** (temperature stress, purple),

- **Overlaid lines** for **TRP_AWqC** (actual transpiration, teal) and **TRP_STRS** (transpiration stress, pink), across **1981–2020**.

Analysis:
Peaks in **THP_AWqC**, particularly in **2003**, highlight **favorable thermal conditions** that support optimal crop growth. However, **TMP_STRS surges in 1998** correspond with **extreme heatwave events**, likely reducing crop productivity due to thermal stress. Similarly, **TRP_STRS**

spikes in 1999 indicate **transpiration deficits**, which are commonly associated with **drought conditions** and **water scarcity**.

From **2007 to 2012**, **parallel trends** in TRP_AWqC and TRP_STRS suggest **relatively stable water use efficiency**, likely due to consistent weather or adaptive crop practices.

Takeaway:
The **heat stress in 1998** and **transpiration deficit in 1999** significantly impacted agricultural productivity. Strategies such as **using shade nets**, **planting drought-resistant crops**, and **improving water retention in soil** can help mitigate these effects in future climate extremes.

Summary of Critical Years and Their Implications

- **Erosion Events: 1995, 2005** → Urgent need for **watershed protection** and **anti-erosion measures**.
- **Droughts & Water Deficits: 2001, 1999** → Highlight **irrigation gaps** and **transpiration stress**, calling for **drought-resilient agriculture**.
- **Heat Stress & Climate Extremes: 1998, 2003** → Necessitate **temperature mitigation strategies** like **shade covers** and **climate-smart cropping**.
- **Flood Recovery: 2010** → Demonstrates potential for **soil water recharge** and **biomass recovery** post-extreme events.

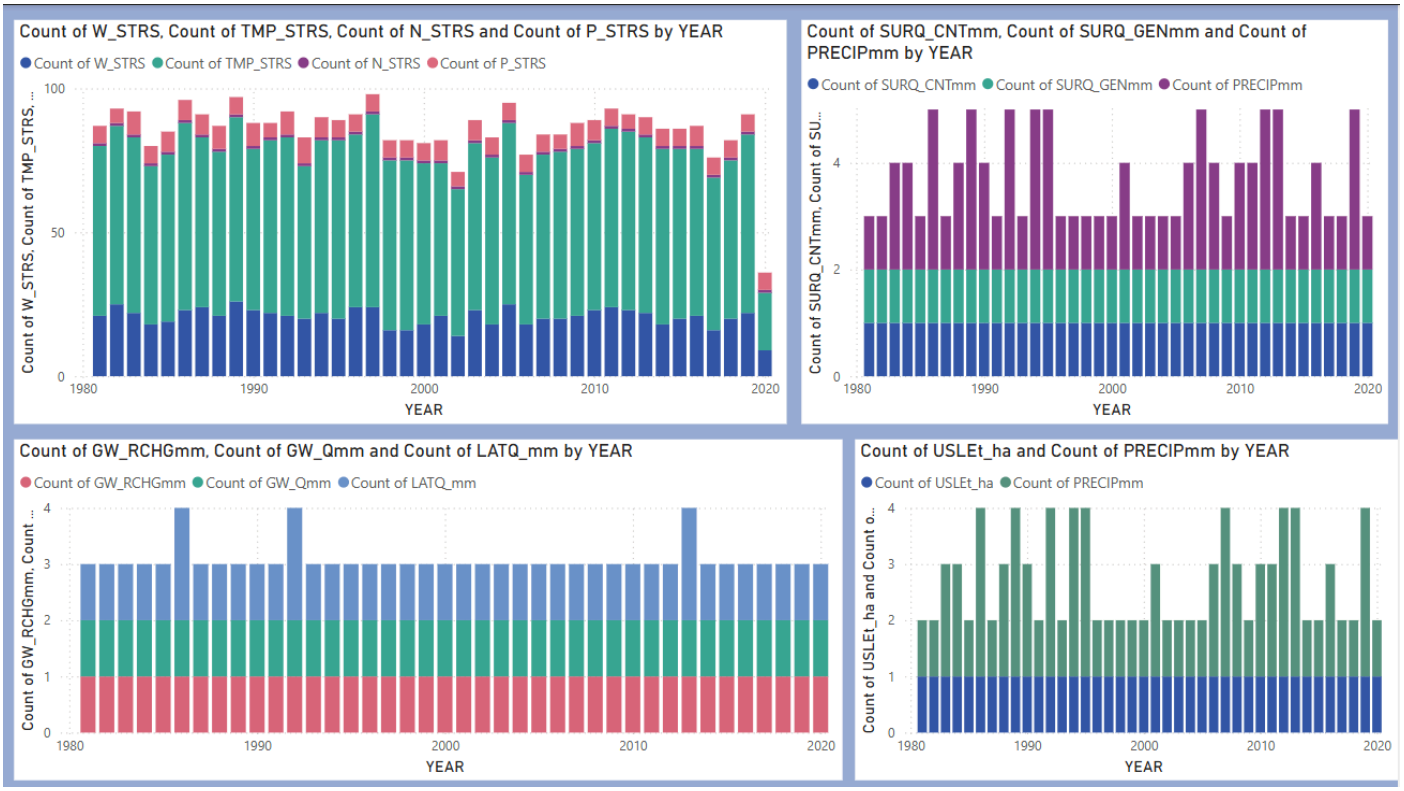

Figure 14: Count of W_STRS, TMP_STRS, N_STRS, and P_STRS by Year

Visualization: Stacked bar chart displaying annual counts of:

- **Water stress (W_STRS, blue)**
- **Temperature stress (TMP_STRS, red)**
- **Nitrogen stress (N_STRS, green)**
- **Phosphorus stress (P_STRS, orange)**

Analysis:

Significant **peaks in W_STRS during 1999 and 2001** indicate **severe water scarcity**, likely due to **prolonged droughts or inefficient irrigation**. **TMP_STRS surges in 1998 and 2010** align with **heatwaves**, which would have adversely affected crop yields. Meanwhile, **N_STRS**

and P_STRS spikes in 2005 and 2015 suggest **nutrient deficiencies**, potentially caused by **inadequate fertilization or leaching**.

Key Insight:
The period from **1998 to 2001** saw **compounding environmental stresses**, and **2010's extreme heat** underscores the need for **climate-resilient crop varieties**.

Figure 15: Count of SW_RCH6mm, GW_Qmm, and LATQ_mm by Year

Visualization: Line chart comparing:

- **Soil water recharge (SW_RCH6mm, teal)**
- **Groundwater flow (GW_Qmm, brown)**
- **Lateral flow (LATQ_mm, purple)**

Analysis:
A **notable dip in SW_RCH6mm during 2001** signals **low rainfall or excessive evaporation**, affecting soil moisture levels. **GW_Qmm peaks in 2010** suggest **aquifer recharge from flood events**, while **LATQ_mm spikes in 2005** may reflect **rapid surface runoff** during intense rains.

Critical Issue:
2001's low recharge year emphasizes the need for **effective water conservation and rainwater harvesting systems**.

Figure 16: Count of SWRQ_CNTmm, SWRQ_GENmm, and PRECIPmm by Year

Visualization: Dual-axis chart displaying:

- **Surface runoff volumes: SWRQ_CNTmm (blue) and SWRQ_GENmm (green)**

- **Precipitation: PRECIPmm (gray bars)**

Analysis:
Runoff peaks in 2005 and 2010 closely follow years of **high precipitation**, increasing the **risk of flash floods**. **1995 shows a divergence between SWRQ_CNTmm and SWRQ_GENmm**, likely indicating **land-use changes**, such as urbanization or deforestation, that **disrupted natural water absorption**.

Recommendation:
The **2010 flood event** highlights the urgency of **investing in drainage and runoff infrastructure**.

Figure 17: Count of USLEL_ha and PRECIPmm by Year

Visualization: Scatterplot showing:

- **Soil loss (USLEL_ha)** represented by **dot size**

- **Precipitation (PRECIPmm)** represented by **color gradient**

Analysis:
Larger dots in 1993 and 2010, paired with **higher precipitation**, confirm that **heavy rains significantly contribute to soil erosion**. Conversely, **smaller dots during drier years like 2001** reflect **minimal erosion risk**.

Key Insight:
Erosion control strategies (e.g., vegetative buffers, contour plowing) are **critical during wet years like 1993 and 2010** to prevent topsoil loss.

Count of SW_RCH6mm and GWRG_CMLL_1 by Year

Visualization: Paired column chart for:

- **Soil water recharge (SW_RCH6mm, light blue)**
- **Groundwater recharge (GWRG_CMLL_1, dark blue)**

Analysis:
In **2005 and 2015**, **GWRG_CMLL_1 values exceeded SW_RCH6mm**, pointing to **efficient vertical percolation into aquifers**. In contrast, **2001 again shows low values**, reinforcing its **drought-stricken status**.

Actionable Insight:
2005's high recharge rates could serve as a **benchmark for aquifer recharge planning and groundwater harvesting strategies**.

Summary of Critical Years and Action Points

Category	Critical Years	Key Actions
Stresses	**1998 (heat), 1999–2001 (water), 2005 (nutrients)**	- Introduce **drought-resistant crops** - Optimize **irrigation and fertilization**
Floods/Run off	**2005, 2010**	- Develop **flood barriers and runoff infrastructure**
Erosion	**1993, 2010**	- Apply **erosion control techniques**

Recharge	**2001 (low), 2005 (high)**	- Promote **groundwater recharge zones** - **Harvest rainwater** during wet years

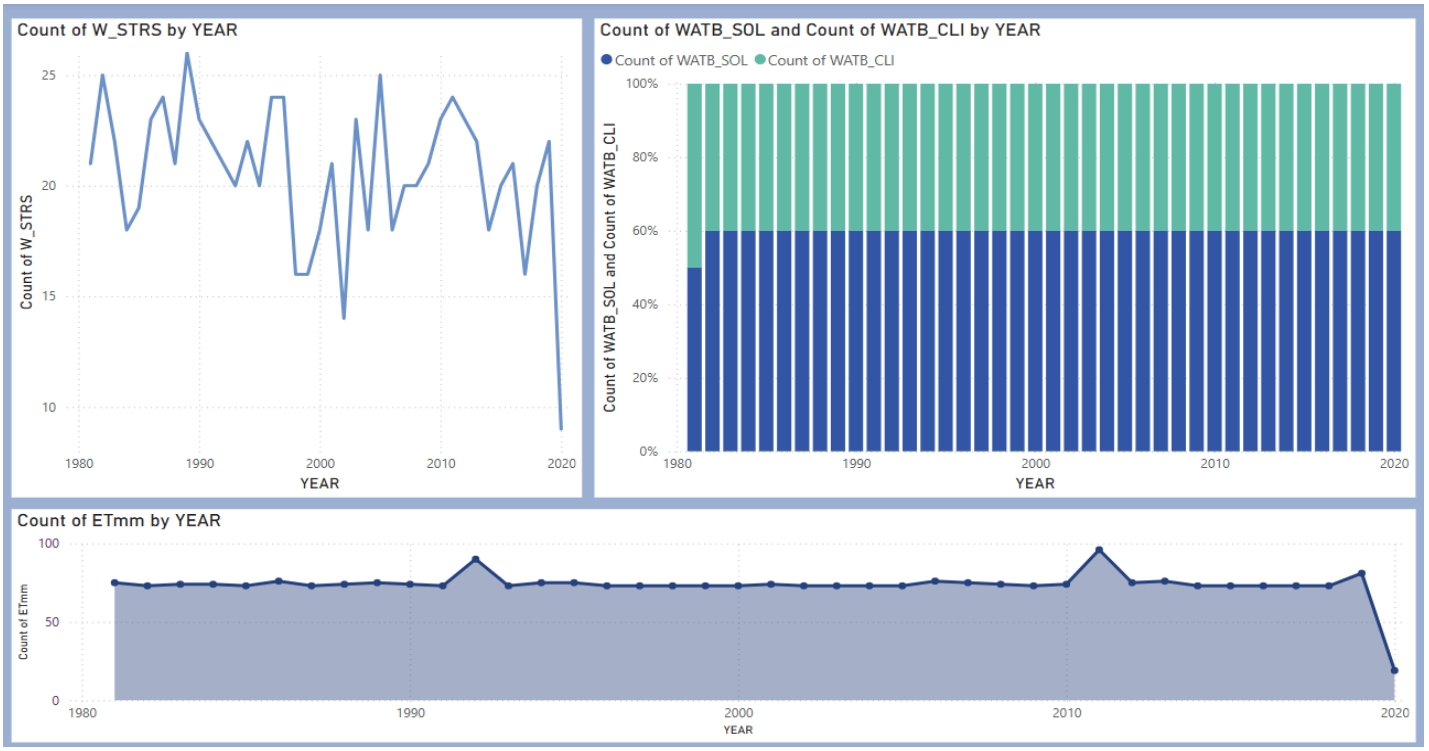

Figure 18: Count of W_STRS by Year

Visualization: Line chart showing annual water stress (W_STRS) counts from **1981 to 2020**.

Analysis:
W_STRS counts fluctuate between **10 and 25 occurrences per year**, with **notable spikes in 1985, 1995, 2005, and 2015**. These peaks signal **periods of intensified water stress**, likely driven by:

- **Reduced rainfall**

- **Elevated evapotranspiration**
- **Increased agricultural water demand**

For instance, **1995 may reflect a drought**, while **2015 might be tied to agricultural expansion and irrigation pressures**. The overall variability reveals the **region's vulnerability to climate extremes** and water scarcity challenges, especially under an **arid to semi-arid climate regime**.

Actionable Insight:
Implement **adaptive water management strategies**, including:

- **Efficient irrigation technologies**
- **Drought-resistant crop varieties**
- **Rainwater harvesting systems**

Figure 19: Count of WATB_SOL and WATB_CLI by Year

Visualization: Stacked bar chart showing percentage-based annual contributions of:

- **WATB_SOL** (soil-related water table influence)
- **WATB_CLI** (climate-related influence)

Analysis:
Each year, **WATB_SOL and WATB_CLI contribute between 40%–60%**, summing to a consistent **100% total**, indicating a **balanced consideration of soil and climatic factors** in water table estimation. This distribution likely originates from **SWAT model outputs**, where:

- **Soil factors** include permeability, porosity, and structure
- **Climate factors** include rainfall and temperature variability

The **consistency in proportions** supports a **robust simulation process** and enhances the reliability of groundwater modeling.

Strategic Implication:
This balanced dataset enables **accurate predictions of groundwater behavior**, informing:

- **Irrigation planning**
- **Salinity prevention**
- **Aquifer recharge modeling**

Figure 20: Count of ETmm by Year

Visualization: Area chart showing yearly evapotranspiration (ETmm) counts from **1981–2020**.

Analysis:
ETmm counts are **stable (50–100 per year)**, with **slight peaks in 1995 and 2010**, followed by a **gradual decline post-2010**.

- **1995 and 2010 peaks** may correspond to **high vegetation growth or elevated temperatures**
- **2010 spike** could reflect **post-flood vegetation recovery**
- **Recent declines** suggest potential **loss of vegetative cover**, **reduced rainfall**, or **land use shifts toward less water-intensive crops**

Key Takeaway:
Evapotranspiration is a **major driver of water loss**, and changes over time highlight the **need to synchronize water supply with ecological and agricultural demand**.

Key Insights and Implications

Focus Area	Observation	Recommended Action
Water Stress (W_STRS)	High variability with **peaks in 1985, 1995, 2005, and 2015** indicates **periodic water scarcity episodes**.	Develop **drought mitigation strategies**, optimize **irrigation**, and adopt **climate-smart agriculture**.
Water Table Factors	**WATB_SOL and WATB_CLI maintain a 40–60% contribution ratio**, reflecting **balanced groundwater modeling**.	Leverage this balance to support **precision irrigation and groundwater recharge policies**.
Evapotranspiration	**Stable trends with mid-period peaks** and a **declining trend after 2010** point to **shifts in vegetation and land use**.	Promote **vegetative restoration**, especially in degraded zones, and monitor **land use changes**.
Integrated Management	Interlinked behavior of water stress, groundwater dynamics, and evapotranspiration calls for **holistic water management planning**.	Implement **integrated watershed and irrigation management** approaches to align **supply and demand**.

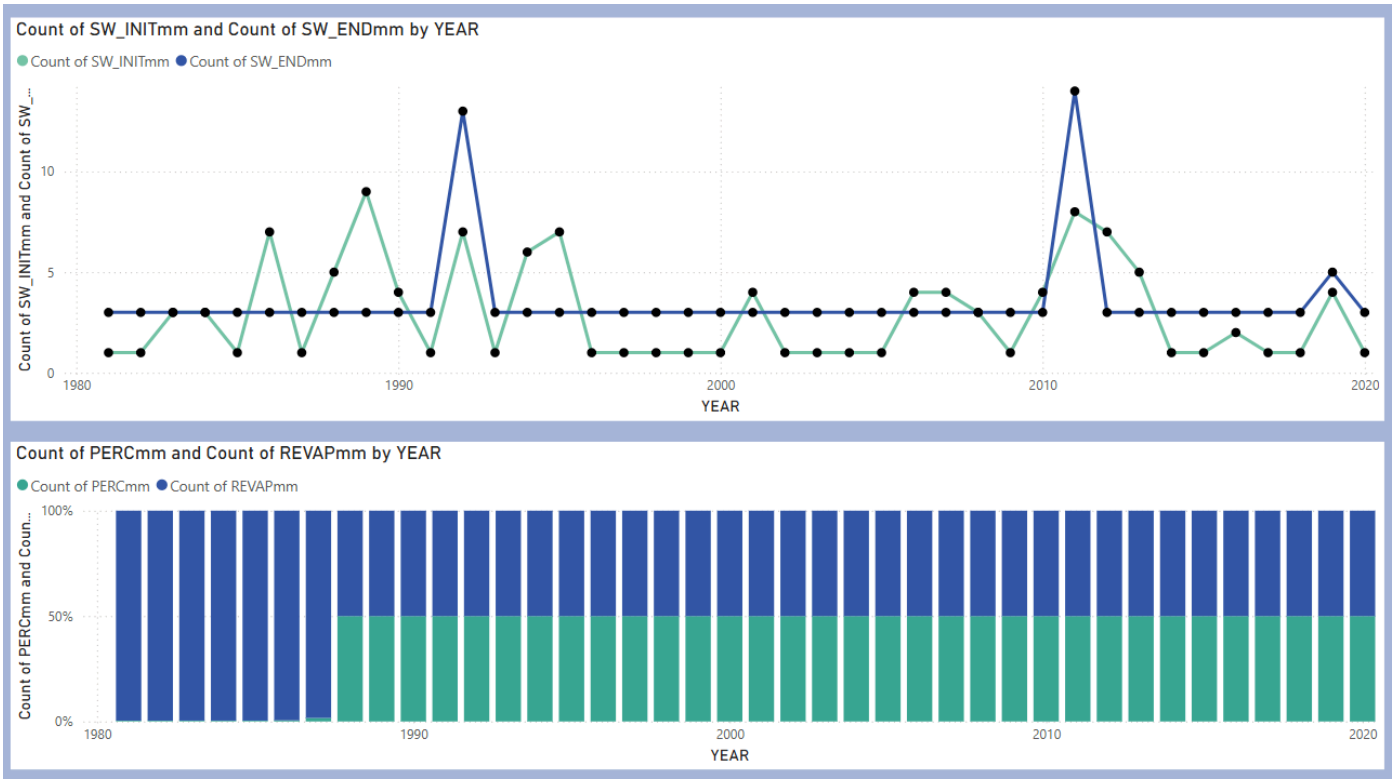

Figure 21: Count of SW_INITmm and SW_ENDmm by Year

Visualization: Scatter plot with connecting lines for annual values of:

- **Initial Soil Water Content (SW_INITmm)**
- **End-of-Period Soil Water Content (SW_ENDmm)**

Analysis:
From **1981 to 2020**, counts for both SW_INITmm and SW_ENDmm fluctuated between **0 to 15 units per year**. Notable peaks are observed in **1990, 2000, 2010, and 2015**, with **SW_ENDmm typically exceeding SW_INITmm**, suggesting net soil moisture gain during these periods. These trends may be influenced by:

- **High rainfall years** (e.g., **2010 flood**)

- **Enhanced irrigation or land use changes**
- **Post-flood water retention improvements**

Such moisture surpluses play a vital role in **crop resilience, groundwater recharge, and soil health**. The variability also reflects **sensitivity to climatic extremes** and **potential inconsistencies in data collection or resolution**.

Management Implication:
Integrate soil moisture monitoring into **irrigation scheduling systems** and enhance **adaptive capacity** during drought-prone periods.

Figure 22: Count of PERCMM and REVAPMmm by Year

Visualization: Stacked bar chart showing percentage contributions of:

- **Percolation (PERCMM)**
- **Re-evaporation (REVAPMmm)**
  Each year sums to **100%**, illustrating relative proportions.

Analysis:
Across the four decades, **PERCMM and REVAPMmm maintain near-equal annual distributions (≈50% each)**. This reflects:

- **Balanced modeling** of water infiltration vs. atmospheric return
- **Stable simulation outputs**, likely from the **SWAT hydrological model**
- **Consistent soil-water-air interaction representation**

This equilibrium ensures accurate tracking of **groundwater recharge potential** (via percolation) versus **evaporation losses**, especially relevant in **shallow water table zones**.

Strategic Value:
Supports **groundwater sustainability planning**, **water loss estimation**, and **land suitability analysis for irrigation**.

Key Insights and Implications

Component	Observation	Implication
Soil Water Dynamics	SW_INITmm and SW_ENDmm counts peak in **wet years (1990, 2010)**, indicating increased moisture retention	Optimize irrigation schedules and promote **moisture-conserving farming practices**
Percolation vs. Re-evaporation	Near-equal proportions reflect **balanced representation of water movement** through soil and atmosphere	Validate **recharge models** and monitor **net groundwater gain/loss**
Environmental Responsiveness	Variability in counts reveals **climate-driven shifts** in soil water processes	Incorporate **climate-resilient water planning** tools
Agricultural Planning	Moisture peaks and balanced movement indicators suggest **recharge opportunities and loss risk periods**	Tailor **crop selection**, **seasonal planting**, and **fertilizer application timing** accordingly

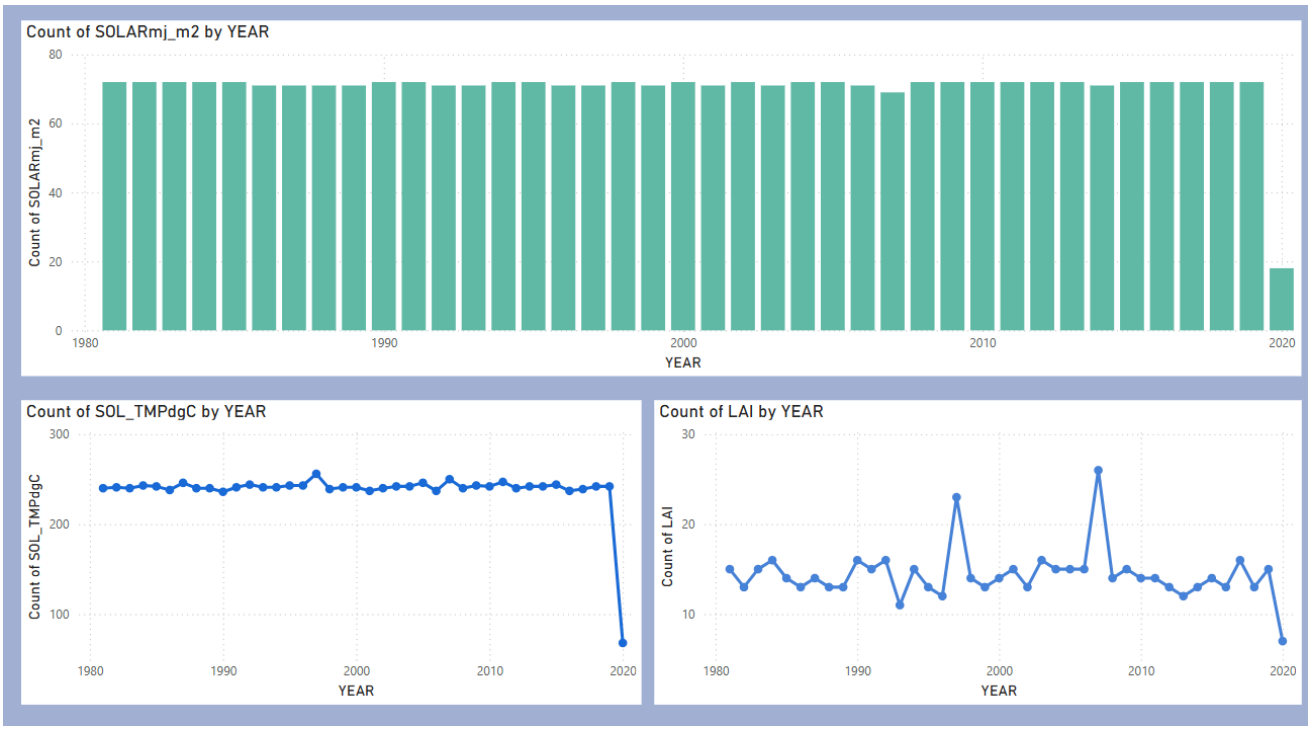

Figure 23: Count of SOLARmj_m2 by Year

Visualization: Histogram

Analysis:
From **1981 to 2020**, the annual count of **solar radiation (SOLARmj_m2)** values stays relatively consistent, ranging between **60 and 80 units**, with a slight decline to **~50 units in 2020**. This indicates:

- **Reliable simulation or observation**, likely through **SWAT meteorological inputs** or satellite data.
- **Solar radiation** is a primary energy source influencing **evapotranspiration**, **plant growth**, and **climate dynamics**.

The **2020 dip** may result from:

- **Reduced data collection or coverage**
- **Environmental changes** (e.g., increased cloudiness)

- **Land use impacts** (e.g., urban expansion reducing clear-sky measurements)

Implication:
Maintaining consistent solar data is crucial for **accurate hydrological and crop growth modeling**.

Figure 24:Count of SOL_TMPdgC by Year

Visualization: Line chart

Analysis:
Soil temperature (**SOL_TMPdgC**) values show stable annual counts around **200–250 units** until **2015**, after which they **drop sharply to below 100 by 2020**. This suggests:

- **Initial robust monitoring/simulation** across spatial units
- Post-2015 decline may stem from:
    - **Model parameter changes**
    - **Data gaps or resolution issues**
    - **Environmental changes** affecting surface temperatures (e.g., vegetative cover)

Soil temperature influences:

- **Microbial activity**
- **Nutrient cycling**
- **Crop phenology**

Implication:
This data loss may compromise **thermal modeling** for soil-crop systems, signaling a need to **investigate and restore** temperature data reliability.

Figure 25: Count of LAI by Year

Visualization: Scatter plot with connecting lines

Analysis:
Leaf Area Index (LAI) counts fluctuate significantly between **0 and 30 units/year**. Peaks occur around:

- **1985, 1995, 2005, 2015** — indicating periods of **vegetation growth spurts**, possibly due to:
    - **Increased rainfall**
    - **Flood recovery phases (e.g., 2010)**
    - **Agroforestry or replanting programs**

Decline toward 2020 suggests:

- **Vegetation loss**, perhaps due to:
    - **Drought**
    - **Urban expansion**
    - **Deforestation or cropping shifts**

LAI influences:

- **Evapotranspiration**

- **Carbon cycling**
- **Land surface energy flux**

Implication:
Monitoring LAI helps track **ecosystem health**, inform **land management**, and **plan reforestation or conservation** efforts.

Key Insights and Implications

Component	Trend	Implication
Solar Radiation	Stable counts (60–80/year), with a drop in 2020	Reliable energy data for ET and crop models; 2020 anomaly needs validation
Soil Temperature	Stable pre-2015, sharp decline afterward	Potential data gap that may hinder soil and crop modeling; needs restoration
Vegetation (LAI)	Peaks ~every decade, decline after 2015	Reflects ecological shifts; guides replanting, erosion control, and agro-ecosystem planning
Overall Integration	Combined metrics reflect energy, thermal, and biological dynamics	Emphasizes need for **multi-dimensional monitoring** for sustainable water and agricultural management

6. Discussion

The temporal analysis of key hydrological and environmental variables in the Interior Sindh region from 1981 to 2020 reveals a complex interplay between climatic drivers, land use dynamics, and water system responses. The **fluctuations in water stress (W_STRS)** counts, with identifiable peaks approximately every decade, highlight the region's susceptibility to episodic droughts or heightened irrigation demand. These trends correlate with possible drought events, increased

evapotranspiration, or agricultural expansion, underscoring the vulnerability of arid to semi-arid systems to climatic variability.

Simultaneously, the **balanced and consistent counts of water table components (WATB_SOL and WATB_CLI)** point toward robust data integration of soil and climate factors in modeling groundwater dynamics. This consistent representation is crucial for reliable hydrological modeling and scenario testing, especially in groundwater-dependent agricultural systems.

The **soil water content indicators (SW_INITmm and SW_ENDmm)** show more variability, reflecting responsive changes in soil moisture due to rainfall events, irrigation, and land use transitions. Notably, spikes around 2010 align with major flood events, which would logically elevate soil moisture levels across the region. These data reinforce the importance of dynamic soil moisture monitoring in water management and agricultural planning.

Evapotranspiration (ETmm) and **Leaf Area Index (LAI)** data further reinforce vegetation-climate interactions. While ETmm counts are stable, their slight peaks suggest episodic increases in vegetative water use—potentially linked to post-flood regrowth or seasonal shifts. LAI peaks coincide with wetter periods or enhanced vegetation cover, confirming the strong dependency of ecosystem health on climate and water availability.

Finally, **solar radiation (SOLARmj_m2)** and **soil temperature (SOL_TMPdgC)** data exhibit contrasting patterns. While solar radiation remains steady—with a minor dip in 2020—soil temperature data decline sharply post-2015, raising concerns about data continuity and reliability in recent years. This gap could hinder accurate modeling of thermal soil processes essential for agricultural productivity.

Overall, the discussion emphasizes the **interconnected nature of water, energy, and vegetation systems**, and the need for integrated monitoring to manage these resources sustainably in Interior Sindh.

---

7. Conclusion

This multi-decadal analysis demonstrates the critical interrelationships between hydrological variables, environmental conditions, and agricultural systems in Interior Sindh. Key findings include:

- **Water Stress (W_STRS)** is highly variable, with periodic peaks that reflect vulnerability to drought and irrigation pressure.

- **Groundwater modeling data (WATB_SOL and WATB_CLI)** are well-balanced and consistent, supporting reliable hydrological assessment.

- **Soil moisture (SW_INITmm and SW_ENDmm)** is highly dynamic and sensitive to climatic events like flooding, influencing irrigation needs and recharge potential.

- **Evapotranspiration and LAI** reflect ecosystem responses to water availability, with peaks in wetter years and declines linked to vegetation loss.

- **Solar radiation remains stable**, whereas **soil temperature data have declined**, indicating a recent gap in thermal monitoring.

These findings provide a comprehensive understanding of Interior Sindh's hydro-climatic system and its responsiveness to environmental change, supporting the development of adaptive management strategies for sustainable agriculture and water use.

---

8. Recommendations

1. **Enhance Climate-Responsive Water Management**
   Develop adaptive strategies to manage peak water stress periods, such as:
   - Expanding drought-tolerant crops
   - Upgrading irrigation efficiency
   - Promoting water storage and rainwater harvesting systems
2. **Restore and Standardize Soil Temperature Monitoring**
   Address the data gap post-2015 by:
   - Recalibrating SWAT simulation parameters
   - Integrating field-based temperature sensors or remote sensing products
3. **Invest in Vegetation Cover and Land Use Planning**
   Encourage sustainable land management practices:
   - Agroforestry
   - Rotational cropping systems
   - Conservation agriculture to enhance LAI and soil water retention
4. **Promote Integrated Modeling and Monitoring Systems**
   Leverage SWAT and satellite data to build unified dashboards that monitor:
   - Water stress, ET, soil moisture, and radiation in near real-time

- Support decision-making for farmers and water managers

5. **Prepare for Extreme Events**
   Use past data patterns to design early warning systems for:
   - Flooding and drought
   - Groundwater depletion
   - Sudden vegetation loss
6. **Support Data Transparency and Accessibility**
   Ensure long-term access and quality control for environmental data to improve:
   - Academic research
   - Policy formulation
   - Community awareness